Translational Oncology 27 (2023) 101600

Contents lists available at ScienceDirect

Translational Oncology

journal homepage: www.elsevier.com/locate/tranon

Original Research

Identification and Validation of Novel Immunogenic Cell Death- and DNA Damage Response-Related Molecular Patterns Correlated with Immune Status and Prognosis in Hepatocellular Carcinoma

Xiaokai Zhang [#], Jie Wen [#], Guixiong Zhang, Wenzhe Fan, Jizhou Tan, Haikuan Liu, Jiaping Li [*]

Department of Interventional Oncology, The First Affiliated Hospital, Sun Yat-sen University, Guangzhou, China, 510080

ARTICLE INFO

Keywords:
Hepatocellular carcinoma
Immunogenic cell death
DNA damage response
Immunotherapy
Prognosis

ABSTRACT

Immunogenic cell death (ICD) and DNA damage response (DDR) are involved in cancer progression and prognosis. Currently, chemotherapy is the first-line treatment for intermediate or advanced hepatocellular carcinoma (HCC), which is mostly based on platinum and anthracyclines that induce DNA damage and ICD. With the treatment of HCC with immune checkpoint inhibitors (ICIs), it is important to understand the molecular characteristics and prognostic values of ICD and DDR-related genes (IDRGs). We aimed to explore the characteristics of ICD and DDR-related molecular patterns, immune status, and the association of immunotherapy and prognosis with IDRGs in HCC. We identified IDRGs in HCC and evaluated their differential expression, biological behaviors, molecular characteristics, immune cell infiltration, and prognostic value. Prognostic IDRGs and subtypes were identified and validated. *FFAR3, DDX1, POLR3G, FANCL, ADA, PI3KR1, DHX58, TPT1, MGMT, SLAMF6,* and *EIF2AK4* were determined as risk factors for HCC, and the biological experiments indicated that high *FANCL* expression is harmful to the treatment and prognosis. HCC was classified into high- and low-risk groups based on the median values of the risk factors to construct a predictive nomogram. These findings provide novel insights into the treatment and prognosis of HCC and provide a new research direction for HCC.

Introduction

Liver cancer is a common malignancy that caused 906 000 new cases and 830 000 deaths globally in 2020 [1]. HCC is a primary subtype of liver cancer that accounts for approximately 90% of all liver cancer cases [2]. In China, HCC is the second most frequently diagnosed cancer and the most common cause of cancer-related deaths [3]. Liver resection remains the primary strategy for treatment [4], however, the prognosis of patients with HCC remains dissatisfactory because of the high recurrence rate after surgery and poor overall survival (OS) [5]. Unfortunately, HCC is almost always diagnosed at middle or advanced stages when palliative treatment is the only option [6]. These treatments include transarterial chemoembolization and hepatic perfusion chemotherapy, with most chemotherapeutic agents based on platinum and anthracyclines [7], such as cisplatin, oxaliplatin, doxorubicin, and epirubicin, which induce DNA damage and ICD [10].

ICD triggers the immune response against dead cell antigens and is mediated by damage-associated molecular patterns (DAMPs), including surface-exposed calreticulin, secreted ATP, and released high mobility group protein B1 [11]. ICD plays a major role in the tumor microenvironment (TME) by activating the immune system against cancer tumors [10]. DAMPs commonly attract and activate dendritic cells to promote antigen presentation and eventually stimulate specific T-cell responses to kill cancer cells [11]. Thus, the induction of ICD might be an effective strategy for anticancer treatment by combining direct cancer cell killing and antitumor immunity [12]. In addition, novel ICD inducer has been designed and synthesized, and shows obvious anticancer activity in HCC [13]. ICD also involves DDR, endoplasmic reticulum stress, and apoptotic responses [14]. Recent reports have identified some crosstalk between DDR and the immune system [15,16], indicating that DDR is linked to both the innate and adaptive immunity in cancers [17]. In addition to surgery, traditional therapeutic agents, radiation, chemotherapy, and immunotherapy can selectively induce DDR in tumor cells to enhance antitumor drug efficiency [16,18]. ICD and DDR are involved in tumor initiation, metastasis, invasion, and prognosis and induce

* Corresponding author at: Department of Interventional Oncology, The First Affiliated Hospital of Sun Yat-Sen University, No. 58 Zhongshan 2 Road, 510080, Guangzhou, PR China, Tel: +86-20-13352890908. Fax: +86-20-87755766.
E-mail address: lijiap@mail.sysu.edu.cn (J. Li).
[#] These authors contributed equally to this work.

https://doi.org/10.1016/j.tranon.2022.101600
Received 29 August 2022; Received in revised form 6 November 2022; Accepted 30 November 2022

Abbreviations

Alpha fetal protein AFP
Biological process BP
Cellular component CC
Copy number variation CNV
Damage-associated molecular patterns DAMPs
Differentially expressed genes DEGs
DNA damage response DDR
Gene Expression Omnibus GEO
Gene Ontology GO
Gene set variation analysis GSVA
Hepatocellular carcinoma HCC
Immune checkpoint inhibitors ICIs
Immunogenic cell death ICD
ICD- and DDR-related genes IDRGs
Kyoto Encyclopedia of Genes and Genomes KEGG
Least absolute shrinkage and selection operator LASSO
Liver, cancer-RIKEN, JP project LIRI-JP
Molecular function MF
Overall survival OS
Principal component analysis PCA
Protein-protein interaction PPI
The Cancer Genome Atlas TCGA
Tumor microenvironment TME

antitumor immune responses, and the combination of ICD- and DDR inducer and ICIs has recently become the focus. However, the efficacy is still unsatisfactory. The challenges of immunotherapy in HCC are finding predictive biomarkers, advancing early treatment, classifying treatment, and finding more effective combinatorial therapy [19]. Hence, the identification of ICD- and DDR-related molecular subtypes and their responses to immunotherapy in HCC is necessary.

In this study, we investigated ICD- and DDR-related molecular patterns using online databases, namely The Cancer Genome Atlas (TCGA), Gene Expression Omnibus (GEO), and International Cancer Genome Consortium (ICGC). We identified differentially expressed genes (DEGs), biological function, immune cell infiltration, somatic mutations, and prognostic values that informed the construction of a prognostic predictive model using bioinformatics methods and provide a perspective for exploring the diagnosis and treatment of HCC.

Materials and methods

Data information and processing

The mRNA profiles, somatic mutation data, copy alteration data, and corresponding clinical data of 368 tumor samples and adjacent non-tumor samples were downloaded from TCGA (https://portal.gdc.cancer.gov/) and the University of California Santa Cruz Xena browser (https://xena.ucsc.edu/). The mRNA expression profiles and corresponding clinical information in the GSE14520 dataset, containing 225 tumor and non-tumor samples, were obtained from GEO (https://www.ncbi.nlm.nih.gov/geo/) database and generated using the Affymetrix HT Human Genome U133A Array. The Liver cancer-RIKEN, JP project (LIRI-JP) dataset (https://dcc.icgc.org/projects/LIRI-JP), including the mRNA profiles and corresponding clinical information of 240 tumor samples and 198 non-tumor samples, was obtained from the ICGC data portal. We also collected 671 ICD-related genes from previous articles [8,9,12,20] and 451 DDR-related genes from the Molecular Signatures Database (http://www.gsea-msigdb.org/gsea/index.jsp). The differentially expressed IDRGs between HCC tumor and non-tumor samples were visualized using the ggplot package in R.

Selecting prognostic IDRGs and protein-protein interaction (PPI) network construction

The survival package in R and univariate Cox analysis were used to screen the prognostic IDRGs with P-values < 0.01. The connection between prognostic IDRGs was explored by developing a PPI network. Pearson correlation analysis was used to evaluate the correlation among the prognostic genes with a threshold of absolute Pearson coefficient $>$ 0.5 and P-value $<$ 1e-5. The relationship between the significant prognostic genes and survival was determined using the Surv _cutpoint R package.

Consensus clustering

Based on prognostic IDRGs, patients with HCC were classified into distinct ICD- and DDR-related subtypes using the unsupervised clustering method. The number of clusters was determined by consensus clustering using the ConsensusClusterPlus package in R with 1 000 repetitions to ensure the stability of the classifications. Principal component analysis (PCA) was performed on TCGA-LIHC, GSE14520, and LIRI-JP datasets to verify the performance of the classifications. The OS of each subtype was analyzed using the survival package in R.

Gene set variation analysis (GSVA)

GSVA was performed using the GSVA R package to investigate the biological processes of each ICD- and DDR-related subtype. The different biological processes among different subtypes were confirmed using the limma R package with P-value $<$ 1e-5.

Screening the DEGs among subclusters and their biological function analysis

The ICD- and DDR-related DEGs were screened using the limma R package with an absolute log (fold change, FC) $<$ 1 and adjusted P-value $<$ 1e-5. Gene Ontology (GO) annotation, including biological process (BP), molecular function (MF), cellular component (CC), and Kyoto Encyclopedia of Genes and Genomes (KEGG) pathway enrichment were analyzed using clusterProfiler R package to identify the biological functions of intersected DEGs.

Evaluating gene mutation and copy number variation (CNV)

The genetic alterations between the subtypes were investigated using the mutect R package and visualized using the maftools R package. The copy alteration data from the Xena browser was calculated with Genomic Identification of Significant Targets in Cancer (https://www.genepattern.org/modules/docs/GISTIC_2.0) and then the CNV frequency for the subtypes was analyzed.

Estimating immune cell infiltration

The ESTIMATE algorithm was used to evaluate the immune score, stromal score, and tumor purity. The Kruskal– Wallis test was used for differential comparisons of ICD- and DDR-related subtypes. The enrichment scores, which represented the abundance of each immune cell type, corresponding to TCGA-LIHC samples were downloaded from Tumor Immune Estimation Resource 2 (http://timer.comp-genomics.org/). Differences in the expression of immune checkpoint-related genes among subtypes were investigated using the t-test function in the rstatix R package with Holm–Bonferroni correction.

Response to immunotherapy

A submap algorithm was used to predict the response to immune checkpoint inhibitors PD-1 and CTLA4, and response of HCC to ICIs was classified into response and nonresponse. Statistical significance was set at $P < 0.05$.

Prognostic signature and risk model construction

Prognostic IDRGs were incorporated into a least absolute shrinkage and selection operator (LASSO) regression model using univariate Cox analysis to generate a prognostic ICD- and DDR-related gene signature using the glmnet R package. All the samples were classified into high- and low-risk groups based on the median risk score and compared using Kaplan–Meier analysis. A time-dependent ROC curve was used to evaluate the predictive accuracy of the risk model. The Kaplan–Meier analysis and ROX curves were used to validate the predictive ability of the validation cohorts (GSE14520 and LIRI-JP datasets) and ensure the stability of the prognostic signatures.

Development of a nomogram

Univariate and multivariate Cox analyses were performed using the cph function in the rms R package to evaluate the prognostic values of the risk score and clinicopathological characteristics. Based on the risk score and clinicopathological characteristics, a nomogram was developed to predict the prognosis of HCC patients. Calibration plots were constructed to evaluate the accuracy and stability of the predictive models.

Cell culture and siRNA transfection

Huh-7 (human hepatoma cell line, Wuhan Fine Biotech Co., Ltd, Wuhan, China) cells were cultured in Dulbecco's modified Eagle's medium (DMEM, Gibco, CA, USA) containing 10% fetal bovine and 1% penicillin-streptomycin in culture flasks of 25 cm^2 and maintained in a humidified incubator with 5% CO^2 at 37 ℃. The siNC and siFANCL small interfering RNA (siRNA) were transfected into Huh-7 cells with Lipofectamine 2000 transfection reagent (Invitrogen, Carlsbad, CA, USA), respectively. Briefly, Huh-7 cells were randomly divided into the following groups: the siNC group transfected with the scrambled siRNA (negative control) and the siFANCL group transfected with the siRNA specific for FANCL (target sequence GACAAGAGCTGTATGCACT) (Sangon Biotech, Guangzhou, China). Transfection experiments were performed when cells were 50% confluent in six-well plates. Once the cells reached the desired confluence, the culture medium was aspirated, and 1.5 mL complete medium was added to each well. SiRNA (20 nM) and lipo2000 (5 μL) were added to 0.5 mL of the serum-free medium, mixed, and incubated at room temperature for 30 min. The siRNA-lipo2000 mixture was added to each well, and wells were cultured at 37°C in a humidified atmosphere with 5% CO2.

Western blot analysis

The siNC and siFANCL were transfected into Huh-7 cells with Lipofectamine 2000 reagent. After 48 h, western blot analysis was performed. Briefly, cells were lysed with 1% SDS lysing buffer containing protease inhibitor cocktail and phosphatase inhibitor cocktail (Biospec, Inc., Bartlesville, OK, USA). Protein concentration was determined using a BCA protein assay reagent kit (Thermo Scientific, Waltham, MA, USA). All the blots were incubated with primary antibodies for anti-GAPDH (1:5000, Invitrogen, Waltham, MA, USA) and anti-FANCL (1:1000, Cell Signaling Technology, Boston, MA, USA), Protein bands were visualized using ECL reagents (Smart-Lifesciences, Nanjing, China).

Cell growth and viability assay

After the cells were transfected for 48 h, the effect of *FANCL* knockdown and treatment by oxaliplatin on the viability of Hun-7 cells was assessed using the cell counting kit-8 (CCK-8) assay (Songshu Biotech, Guangzhou, China). In brief, the cells were seeded in 96-well plates at a density of 5×10^3 cells per well and cultured for 24 h. Subsequently, the cells were treated with varying concentrations of oxaliplatin (1, 2, 5, 10 μM) for 24, 48, or 72 h. Following this, CCK8 solution (15 μL) were added to each well and incubated for 1 h. Finally, the absorbance of each well was measured at 450 nm using a microplate reader (Thermo Scientific, Waltham, MA, USA). Cell viability (CV) was calculated as follows: $CV=(OD_{test}-OD_{blank})/(OD_{control}-OD_{blank})$.

Clone formation assay

After siNC and siFANCL were transfected into Huh-7 cells for 48 h, they were seeded in a six-well plate at a density of 5000 cells per well and cultured overnight. Then, the cells were treated with the indicated concentrations of oxaliplatin (0 or 1 μmol) for another 14 days. The supernatants were discarded, and the cells were washed three times with phosphate-buffered saline and fixed with methanol for 5 min. Finally, the cells were stained in crystal violet for 20 min, and colonies wre imaged.

Statistical analysis

Data management and statistical analysis were performed using R (version 3.5.3, Vienna, Austria) and GraphPad Prism (version 9.0.0, GraphPad Software Inc., San Diego, CA, USA). All experiments were performed in at least in three biological replicates. Data are presented as the mean ± SD and compared by a one-way ANOVA analysis. Statisitcal significance was set at $P < 0.05$.

Results

Identification of IDRGs with HCC prognostic value

We collected 671 ICD-related and 451 DDR-related genes from the literature and the Molecular Signatures Database (Table S1) and measured the expression of 1,122 IDRGs from HCC samples and non-tumor samples (Fig. 1A). 80 prognostic IDRGs were identified (Table S2), and the top 20 are shown in Fig. 1B. A PPI network was constructed (Fig. 1C). Subsequently, in patients with HCC who presented different expression of the top nine prognostic genes, high expression of *IFNAR1, EIF2AK4, C3, CCR7*, and *PIK3R1* was associated with favorable survival, whereas high expression of *CD58, DDX1, FFAR3*, and *HDAC2* correlated with poor survival (Fig. 1D-L). These results demonstrated that a large proportion of IDRGs, including 80 prognostic genes, are involved in HCC progression.

Construction of ICD- and DDR-related molecular subtypes in HCC

All samples in TCGA-LIHC cohort were classified into three distinct molecular subtypes, i.e., cluster 1 (n=135), cluster 2 (n=152), and cluster 3 (n=81) (Fig. 2A). The expression patterns of these genes are shown in Fig. 2B; there were significant differences in gene expression among the three clusters. PCA showed distinct gene expression profiles among the three subtypes (Fig. 2C), and Kaplan–Meier analysis indicated significant differences in the survival among the three subtypes, with the worst survival in cluster 3 (Fig. 2D). To ensure the stability of the subtypes, we also performed clustering in the validation cohorts (Fig. 2E, G). There was also a distinct survival time among the three subtypes, with cluster 3 having the shortest survival time in the GSE14520 cohort (Fig. 2F); patients in cluster 1 showed a worse survival than those in clusters 2 and 3 in the LIRI-JP cohort (Fig. 2H). We also

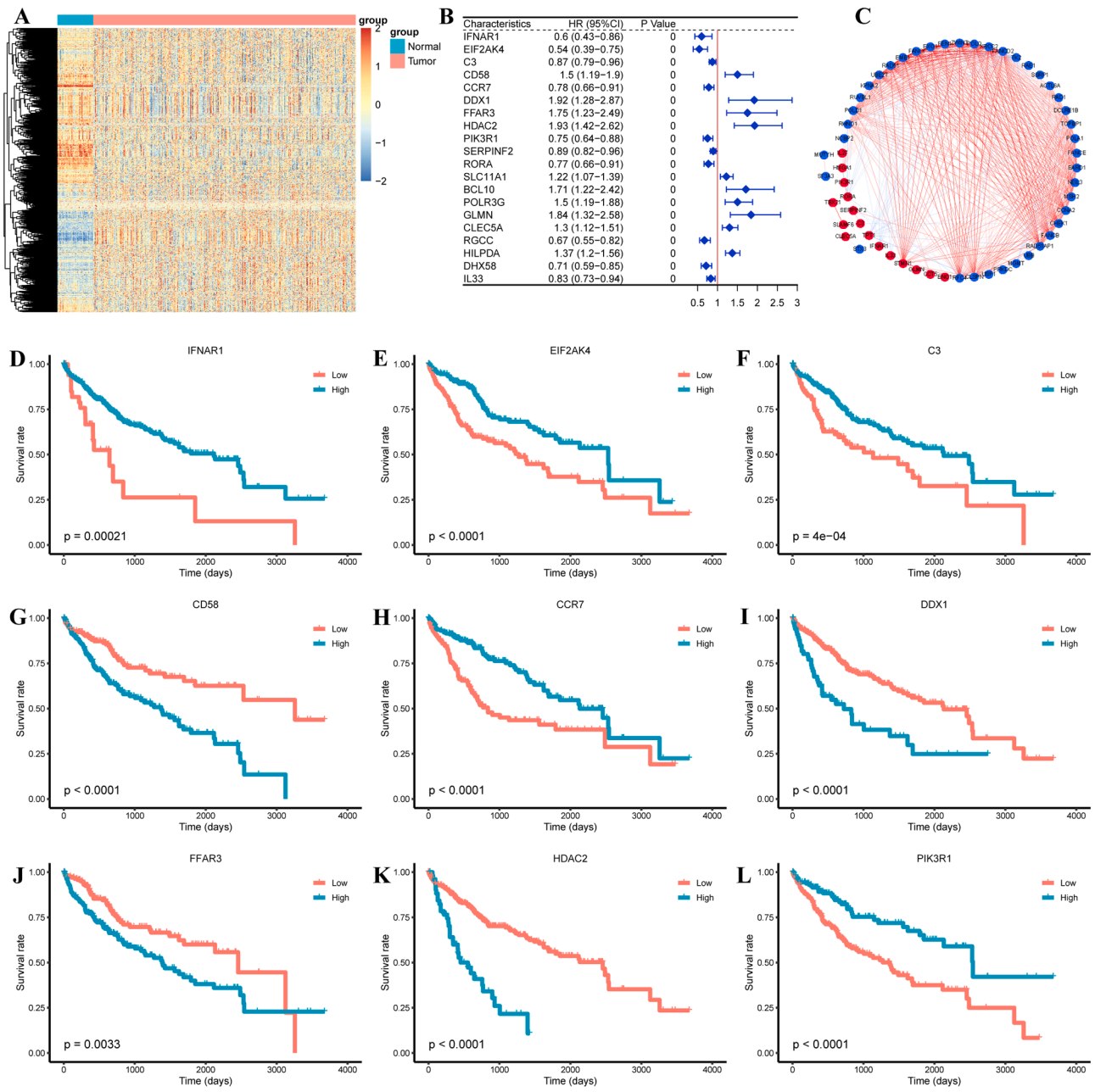

Fig. 1. Identification of nine IDRGs with prognostic value in HCC
(A) Heatmaps illustrating the expression of 1 122 IDRGs in TCGA-LIHC cohort. (B) The top 20 prognostic IDRGs associated with prognosis of HCC patients.(C) A PPI network including 50 prognostic IDRGs with |coefficient| > 0.5 and *P*-value < 1e-5. The red and blue dots represent DDR and ICD genes, respectively.(D)-(L) Kaplan–Meier analysis of the OS of patients with high and low expression of the top 9 IDRGs.

investigated the differences in clinicopathological characteristics within these subtypes, including TCGA molecular clustering, immune-related clustering, vascular tumor cell type, alpha fetal protein (AFP), hepatic cirrhosis, alteration of TP53, clinical stage, age, and sex. These results indicated obvious differences in molecular characteristics, pathological features, and prognosis among the three subtypes.

Transcriptomic and biological function characteristics in ICD- and DDR-related subtypes

GSVA enrichment analysis showed distinct enrichment pathways among the three subtypes, the top three biological pathways were enriched in the three clusters: cell cycle, homologous recombination and DNA replication (Table S3); cell cycle, apoptosis, and DNA replication-related pathways (Table S4); DNA replication, metabolism and biosynthesis (Table S5). We found 80 937 ICD-related and 1 683 DDR-related DEGs clusters 1, 2, and 3, respectively (Fig. S1B, Table S6-8). A total of 39 DEGs intersected among the three subtypes (Fig. S1C). GO enrichment analysis of the intersected DEGs indicated that they were related to BPs, such as organic acid, carboxylic acid, and cellular amino catabolic processes (Fig. S1D, Table S9). MF analysis indicated that these DEGs were related to inhibitor activity of enzymes, endopeptidase, and peptidase functions (Fig. S1E, Table S10), while CC enrichment indicated that the DEGs were enriched in collagen-containing extracellular matrix, platelet dense granule lumen, and platelet dense granule processes (Fig. S1F, Table S11). Finally, KEGG pathway enrichment revealed that these DEGs were involved in complement and coagulation cascades; glycine, serine, and threonine metabolism; and peroxisome

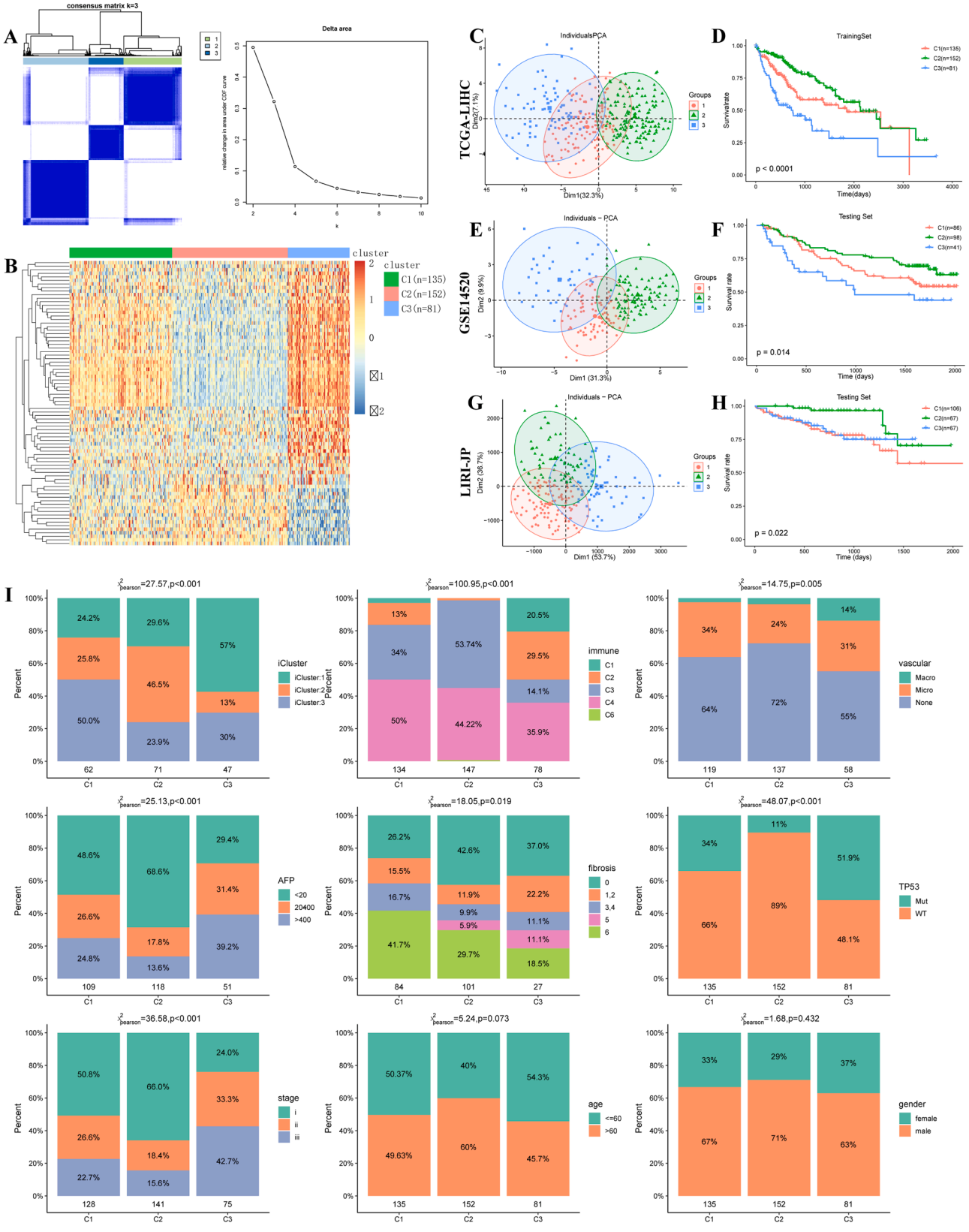

Fig. 2. Construction of three ICD- and DDR-related molecular subtypes in HCC.
(A) Consensus matrix heatmap showing the three subtypes and their correlation to one another. (B) Heatmaps illustrating the expression of 80 prognostic IDRGs in TCGA-LIHC cohort.(C)-(H) PCA for the transcriptome profiles of the three subtypes, with Kaplan–Meier survival curves showing the OS in TCGA-LIHC, GSE14520, and LIRI-JP cohorts, respectively. (I) Rate frequency of the three subtypes in patients was evaluated with TCGA molecular clustering, immune-related clustering, vascular tumor cell type, AFP outcome value, hepatic cirrhosis, alteration of TP53, clinical stage, age, and sex.

pathways (Fig. S1G, Table S12). Together, these results showed differential gene expression among the three subtypes and its association with clinicopathological features and pathway enrichment.

Landscape of genetic alteration in ICD- and DDR-related subtypes

We also investigated the somatic alteration distribution and gene mutation patterns among the three subtypes. which showed that the highest mutation rates of cancer-related genes *TP53* (35%), *CTNNB1* (23%), *MUC16* (22%), and *TTN* (22%) were in cluster 1 (Fig. S2A); *CTNNB1* (32%), *TTN* (26%), *ALB* (14%), *MUC16* (13%), and *PCLO* (13%) were in cluster 2 (Fig. S2B); and *TP53* (54%), *TTN* (28%), and *MUC16* (14%) were in cluster 3 (Fig. S2C). Missense mutations were the most common. We found pervasive CNV changes in the DEGs on

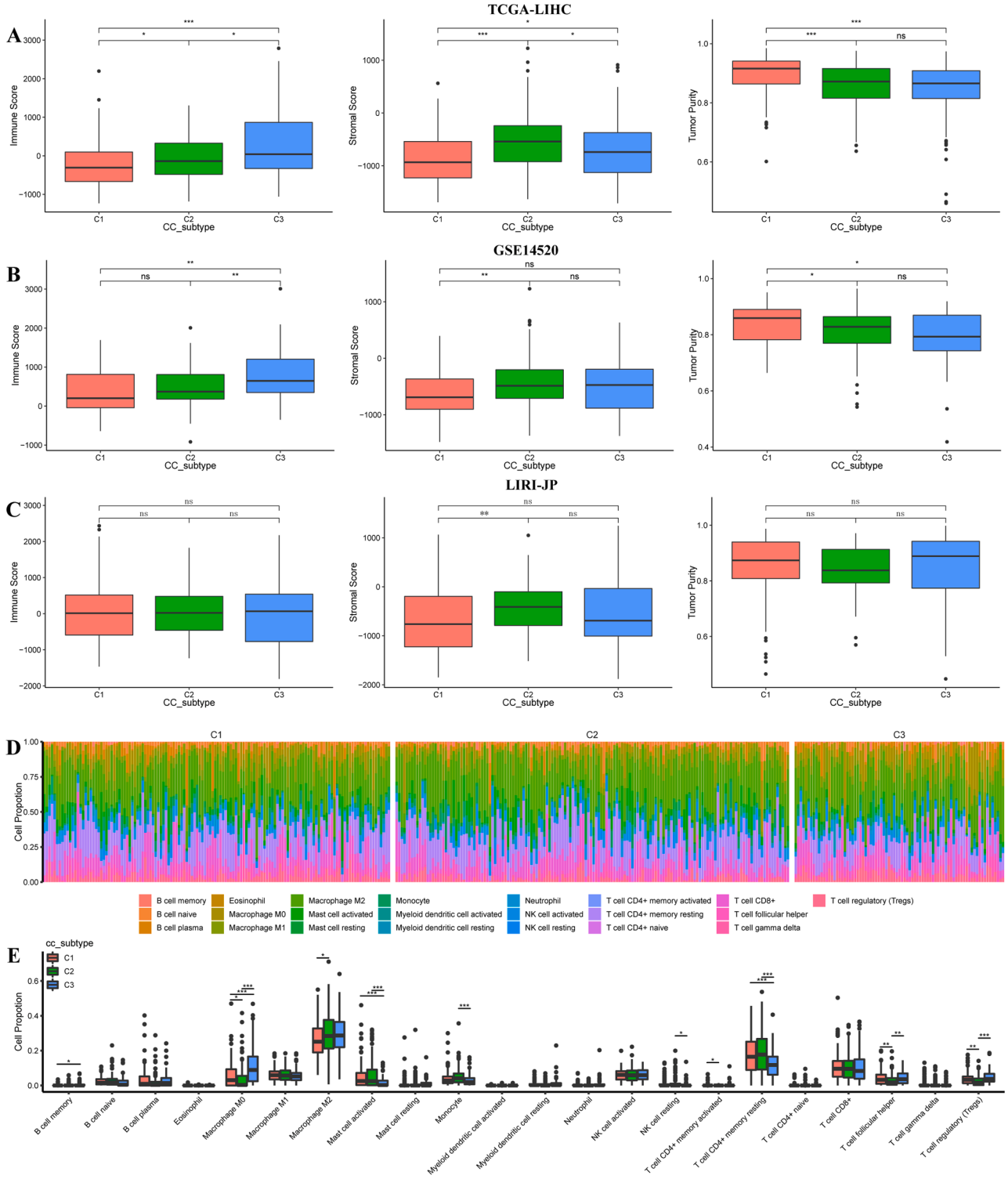

Fig. 3. Infiltration of immune cells into the tumor microenvironment in the ICD- and DDR-related subtypes
(A-C) ESTIMATE algorithm calculated the immune score, stromal score, and tumor purity.(D) Heatmap of the infiltrating immune cells.(E) A box plot of the different immune cell distributions. ns, not significant; $*P < 0.05$; $**P < 0.01$; $***P < 0.001$.

chromosomes in all three subtypes (Fig. S2D), with significant differences in CNV changes among the three subtypes (Fig. S2E).

Tumor microenvironment immune cell infiltration in ICD- and DDR-related subtypes

We further investigated the immune characteristics of subtypes and found that the highest immune score in cluster 3 in TCGA-LIHC, GSE14520, and LIRI-JP datasets (Fig. 3A-C). We explored the immune cell fraction among the three subtypes, and the results showed that Macrophage M0, activated mast cells, resting CD4+ memory T cells, T follicular helper cells (Tfhs), and regulatory T cells (Tregs) were differentially enriched in all three subtypes. Activated mast cells and resting CD4+ memory T cells enriched in clusters 2 than clusters 1 and 3, and Macrophage M0, Tfhs, and Tregs were significantly elevated in cluster 3 (Fig. 3D-E, Table S13-14). The immune cell microenvironment of HCC is complicated, briefly, effector T cells have an overall positive effect, whereas Treg and tumor associated macrophages have a negative effect; in addition, the number and activation status of T cells has influence on tumor response to ICIs [19]. These results suggested that the TME immune cell infiltration in ICD- and DDR-related subtypes are different, which may indicate different responses to immunotherapy.

Response to anti-CTLA-4 and anti-PD-1 treatment in HCC

The landscape of immune cell infiltration among the three subtypes

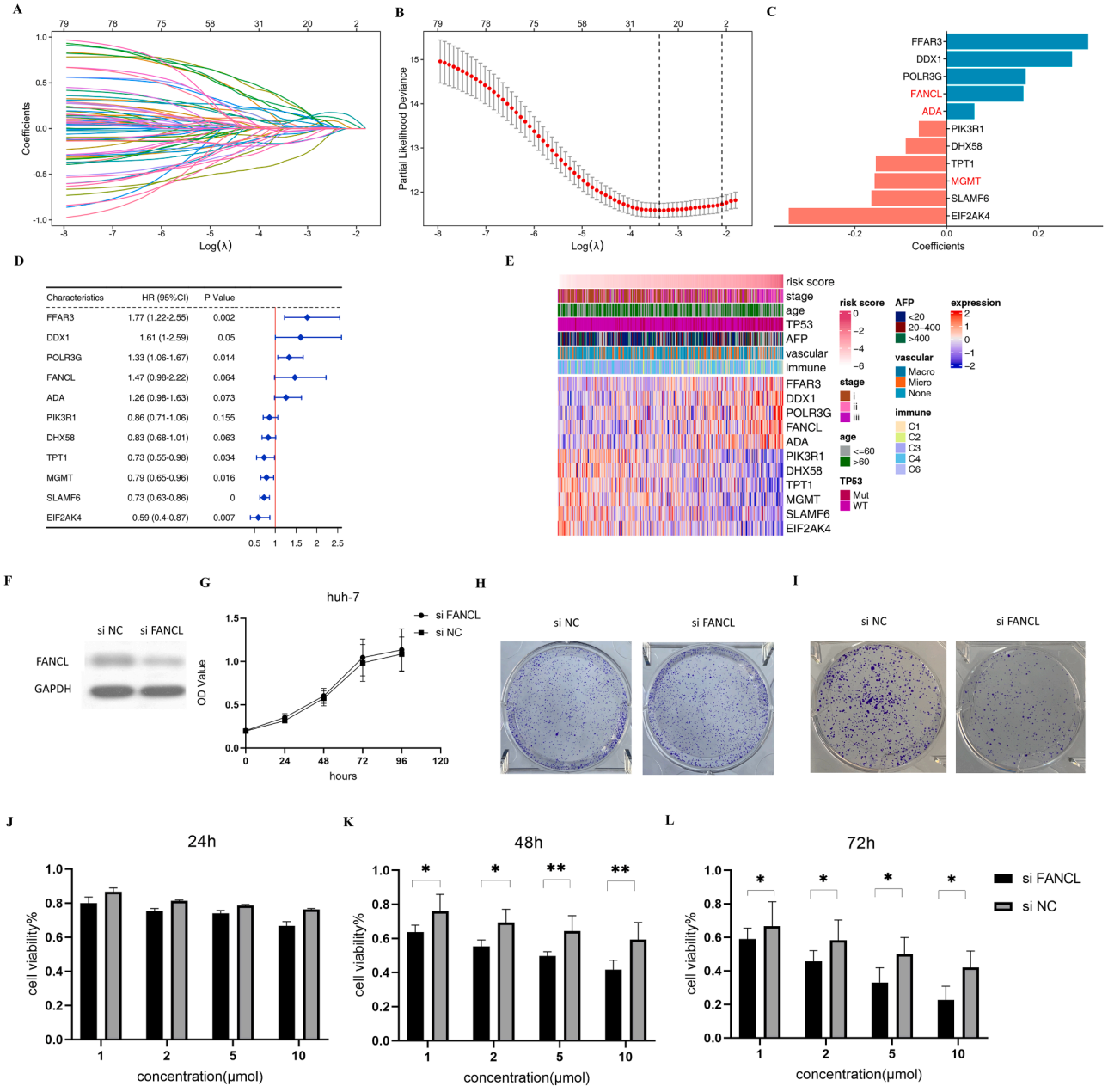

Fig. 4. Construction of an IDRGs signature and function validation in vivo
(A) LASSO coefficient distribution of 21 IDRGs. (B) 10-fold cross-validation error rate. (C) Bar chart showing the coefficients of 11 IDRGs signatures.(D) Forest plot showing the independent factors for prognosis prediction. (E) Heatmap of the correlation between the risk score and IDRGs signature or clinicopathological characteristics. (F) Western bolt analysis confirmed the efficiency of siRNA knockdown of *FANCL*. (G-H) Clone formation and CCK8 assay for cell viability of Huh-7 cells in vitro. The cells were cultured for 24, 48, 72, 96h.(I-L) Clone formation and CCK8 assay for cell viability of Huh-7 cells in vitro by treat withvarying concentrations of oxaliplatin (1, 2, 5, 10 μM) for 24, 48, 72 h. Data shown are mean ± SD of triplicate samples for each treatment. *P*-values are shown as: *, $P < 0.05$; **, $P < 0.01$.

might indicated potentially different responses to immunotherapy. Therefore, we examined the expression of immune checkpoint-related genes and found the difference among the subtypes (Fig. S3A-C). Based on responses to immune checkpoint blockade therapy, significant responses to anti-CTLA4 and anti-PD1 immunotherapy in cluster 2 compared to clusters 1 and 3 were noted (Fig. S3D). These results indicated that the landscape of immune cell infiltration among the three subtypes induced different responses to immunotherapy.

Construction and validation of an ICD- and DDR-related gene signature in HCC

We identified 21 ICD- and DDR-related gene candidates (Fig. 4A-B). After stepwise multivariate Cox regression analysis, a prognostic ICD- and DDR-related gene signature containing 11 genes (*FFAR3, DDX1, POLR3G, FANCL, ADA, PI3KR1, DHX58, TPT1, MGMT, SLAMF6*, and *EIF2AK4*) was generated (Fig. 4C-D). Based on the median value of risk score, 368 samples were classified into high-risk (n= 183) or low-risk (n= 185) groups (Table S15). The heatmap visualization of the risk score analysis showed that high expression of *FFAR3, DDX1, POLR3G, FANCL*, and *ADA* and low expression of *PI3KR1, DHX58, TPT1, MGMT, SLAMF6*, and *EIF2AK4* was more associated with the high-risk group (Fig. 4E). Moreover, analysis of the correlation between risk scores and clinicopathological characteristics indicated that high-risk scores were associated with clinical stage and *TP53* mutations (Fig. 4E, Table S16). In addiation, we performed loss-of-function experiments and silenced the expression of a randomly selected gene, i.e., *FANCL*, in the human HCC cell line Huh-7. Western blotting analysis confirmed the efficiency of siRNA knockdown of *FANCL* (Fig. 4F). CCK8 and clone formation assays showed that *FANCL* knockdown did not significantly affect cell viability *in vitro* (Fig. 4G-H); however, it increased the therapeutic effect of oxaliplatin, indicating that high *FANCL* expression is harmful to the treatment and prognosis of HCC (Fig. 4I-L).

Correlation between clinicopathological characteristics and ICD- and DDR-related risk score

ICD- and DDR-related subtypes were significantly associated with risk scores in the TCGA-LIHC, GSE14520, and LIRI-JP cohorts and a high-risk score indicated poor survival time for patients with HCC (Fig. 5A-B). These results were consistent with those from cluster 1 in both the training and validation cohorts (Fig. 5C-E), and time-dependent ROC curves verified the predictive probability for 1-5 years of survival in patients with HCC (Fig. 5F). These findings suggested that IDRGs profiles are useful in the prediction of disease prognosis.

Construction of a predictive nomogram for HCC

The univariate and multivariate Cox regression models demonstrated that risk score, stage, sex, vascular, age, and AFP were independent prognostic variables for HCC, and the risk score had the best predictive prognosis accuracy (Fig. 6A-B). Therefore, a nomogram was constructed based on these independent variables (Fig. 6C), and the calibration curves for survival probability at 1 and 3 years indicated the predictive ability of the model (Fig. 6D-E). Together, these results showed that the nomogram based on the ICD- and DDR-related risk score can be used as a quantitative analysis tool to predict the survival risk of HCC patients.

Discussion

There were some new foundings in this study. First, we identified and validated a ICD- and DDR-related gene signature and a predictive nomogram containing 11 genes for the prediction of HCC; Furthermore, we constructed of ICD- and DDR-related molecular subtypes and found the immune features and the different responses to immunotherapy, providing scientific references for clinical immunotherapy.

The mutational landscape of DDR genes in HCC has been identified and suggests that some mutations may be promising targets for precision cancer treatment [21], with DDR serving as a potential biomarker for predicting the clinical potential of immunotherapy and non-immunotherapy in HCC [22]. ICD is an important pathway that can be induced by DNA-damaging drugs and is linked to DDR during the antitumor immune response by triggering antigen and adaptive immune responses, in addition to activating cytotoxic T cells [8]. Evidence has suggested that targeting DDR promotes the high cytotoxicity in HCC through ICD arising in response to DNA damage [23]. Therefore, finding novel molecular biomarkers can improve the effectiveness of treatment strategies and indicate prognosis in HCC.

Thus, we investigated the expression and prognostic value of IDRGs in HCC and used this transcriptional information to divide HCC samples into three ICD- and DDR-related subtypes, to explore the transcriptomic and biological function characteristics, landscape of genetic alteration, immune features, immunotherapy response and the different prognoses in these subtypes. We comprehensively investigated the molecular characteristics of ICD- and DDR-related subtypes and found 39 DEGs among the three subtypes. These genes inhibit or activate several enzymes and are involved in some biological functions, including complement pathways, a key component of innate immunity and is associated with carcinogenesis and HCC development by promoting immunosuppressive, stimulant, and angiogenic microenvironments [24]. We found that the metabolism of glycine, serine, and threonine was differentially regulated in the ICD- and DDR-related subtypes in patients with HCC. Peroxisomes are involved in lipid metabolism and cellular redox balance, targeting lipid metabolism promotes ICD and links DDR to metabolism, whereas lipid metabolic alterations regulate the DDR pathway [25,26].

Somatic alteration analysis indicated that the mutation rates significantly differed between the three subtypes. Somatic mutations in *TP53* are the most frequent alterations in human cancers, affect the progression and prognosis of HCC, and are associated with the immune microenvironment in HCC [27,28]. *CTNNB1* mutations are also frequently found in HCC, where they promote Wnt/β-catenin pathway activation and facilitate tumor progression; therefore, *CTNNB1* mutations can be used as biomarkers for evaluating immunotherapeutic effect in HCC [29–31]. *MUC16* is a novel oncogene in cancers that is strongly related to tumorigenicity and antitumor therapy resistance [32]. It suggested that the distinct mutation landscape among the ICD- and DDR-related subtypes might indicate different clinical outcomes for HCC treatments.

ICIs, including programmed cell death-1 (PD-1 or its ligand PD-L1) and CTLA-4, have become established pillars in the treatment of advanced HCC [33]. DNA damage could induce antitumor immunity, and DDR pathway blockade might affect PD-L1 expression [34]. DDR inhibition may selectively sensitize innate immune signaling and ICD and potentiate antitumoral cytotoxic T cells [35,36]. DDR-targeted ICD may increase the efficacy of PD1 blockade and sensitize ICI-refractory tumors [37,38]. Some approaches based on DDR and ICD have shown promising clinical efficacy and have been approved for non-small cell lung cancer, small cell lung cancer, and triple negative breast cancer [39–41]. We found different expression levels of immune checkpoint-related genes among the three ICD- and DDR-related subtypes. Thus, we divided the response of HCC to ICIs into response and nonresponse based on a previous study evaluating the therapeutic efficacy of PD-1 and CTLA-4 inhibitors in melanoma [42], and our analysis indicates that patients in cluster 2 showed more sensitivity to anti-CTLA4 and anti-PD1 treatment. That provide new insights into the classification and precise immunotherapy for HCC.

We identified a prognostic ICD- and DDR-related gene signature containing 11 genes, and further analysis showed that high expression of *FFAR3, DDX1, POLR3G, FANCL*, and *ADA*, and low expression of *PI3KR1, DHX58, TPT1, MGMT, SLAMF6*, and *EIF2AK4* was more

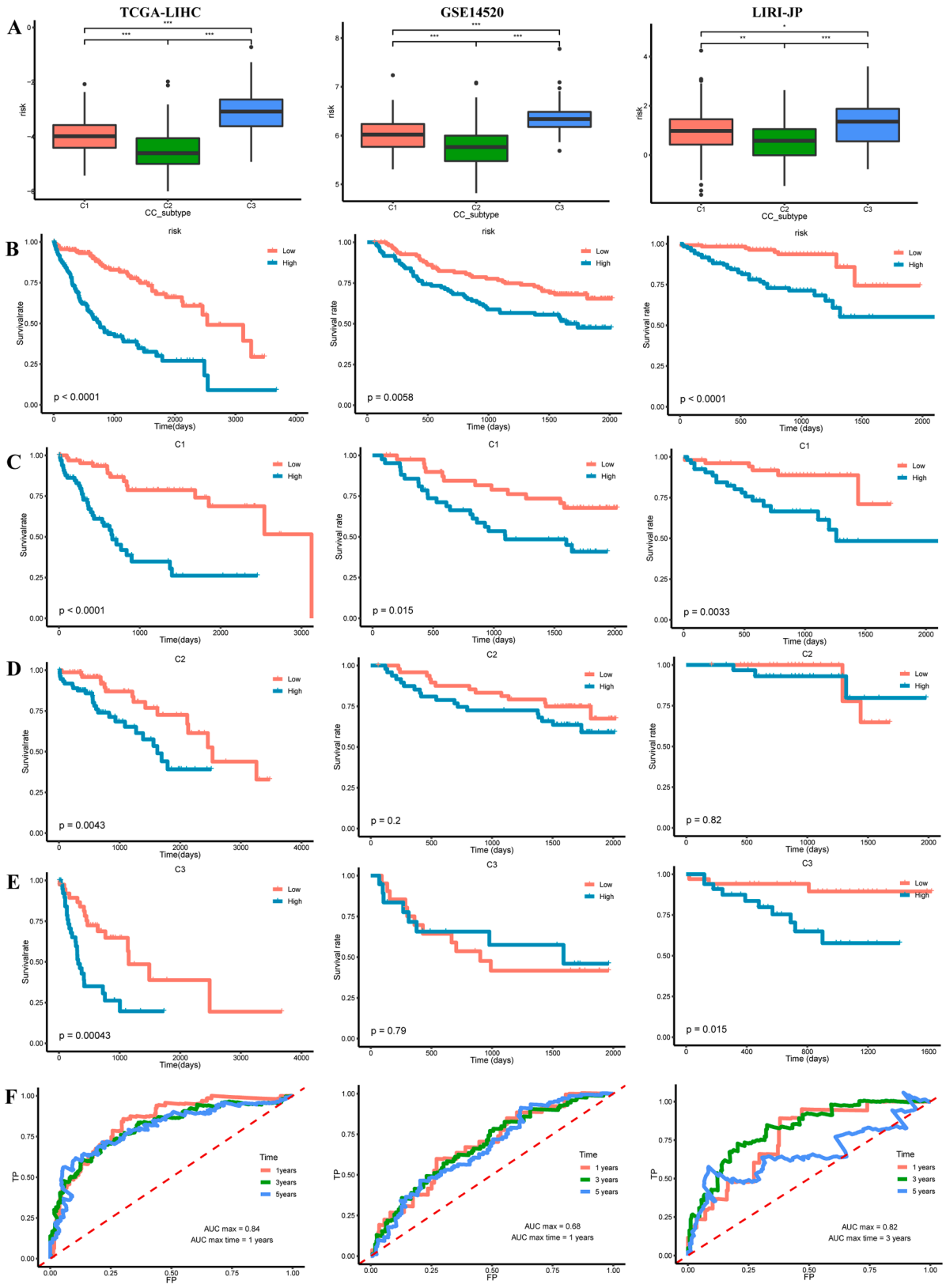

Fig. 5. Correlation between clinicopathological characteristics and ICD- and DDR-related risk score
(A) Box plots showing the correlation between risk score. ns, not significant; *$P < 0.05$; **$P < 0.01$.; *** $P < 0.001$.(B-E) Kaplan–Meier analysis of the relationship between risk score and OS in patients.(F) Time-dependent ROC curves showing the predictive value of the risk score for 1-, 3-, and 5-year OS.

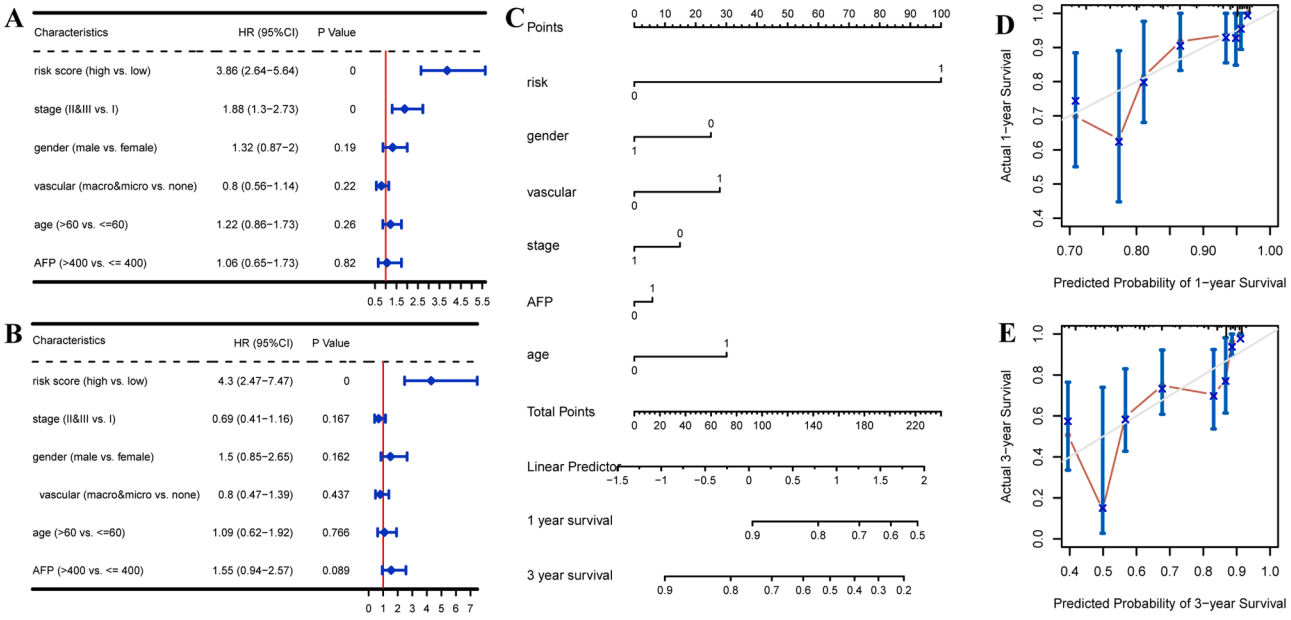

Fig. 6. Construction of a predictive nomogram for HCC
(A-B) Forest plots of the independent factors established by incorporating the risk scores and clinicopathologic characteristics. (C) A nomogram for 1-, 3-, and 5-year survival prediction.(D-E) Calibration curves illustrating the predicted probability of 1- and 3-year survival in patients with HCC.

associated with the high-risk group. The prognostic value of *DDX1, POLR3G, ADA, MGMT, SLAMF6* and *EIF2AK4* in HCC have been reported [43–48]. We silenced the expression of *FANCL*, and investigated its biological function in the human HCC cell line Huh-7 by performing loss-of-function experiments. We found *FANCL* knockdown increased the therapeutic effect of oxaliplatin in HCC. Studies showed that high *FANCL* expression was a risk factor for tumor prognosis and related to chemotherapy resistance in prostate and breast cancers [49,50]. Our data also indicated that the high expression of *FANCL* is harmful to the treatment and prognosis of HCC. However, the biological function and molecular mechanisms underlying the role of other genes in HCC still need further investigation.

Finally, we investigated the prognostic and predictive values of IDRGs by generating risk and nomogram models. The results indicated that high-risk patients had poorer survival than low-risk patients. Risk score, clinical stage, sex, vascular invasion, age, and AFP level were identified and validated as independent variables that can predict the probability of survival.

This study had some limitations. First, patients in the TCGA-LIHC, GSE14520, and LIRI-JP cohorts may have been administered a variety of antitumor therapies, which could have potentially affected our results. Further validation studies are needed to support the predictive abilities of the identified gene candidates. Future studies should include patients with HCC receiving ICI treatment to further verify the influence of ICD and DDR molecular types on patient outcomes.

Conclusions

We found that the ICD- and DDR-related molecular subtypes and the molecular and immune cell infiltrating characteristics can guide precise HCC immunotherapy, and the prognostic model based on IDRGs was generated to predict the survival time of patients with HCC. These findings may provide a novel method for advancing cancer therapy and evaluating the prognosis of patients with HCC.

Authors' contributions

JL, XZ, and WF contributed to the conception of the study and conceived and designed the experiments. JL supervised the study. XZ, JW, and HL performed the experiments and data analyses and wrote the manuscript. JT contributed to the Discussion and reviewed the manuscript. All authors read and approved the final version of the manuscript.

Ethics Approval and Consent to Participate

Not applicable.

Funding

This study was supported by the National Natural Science Foundation of China (grant numbers 81971719, 82172036, and 81171441); the Major Scientific and Technological Project of Guangdong Province (grant numbers 2020B0101130016); the Guangdong Medical Science and Technology Research Fund (grant number A2020081); and the Key Research and Development Project of Guangzhou City (grant number 202103000430010086).

Declaration of competing interest

The authors declare that they have no competing interests.

Acknowledgements

The authors thank TCGA, GEO, and ICGC repositories for sharing their data, as well as the R development team and the R community for contributing the statistical packages.

Supplementary materials

Supplementary material associated with this article can be found, in the online version, at doi:10.1016/j.tranon.2022.101600.

References

[1] H. Sung, J. Ferlay, R.L. Siegel, M. Laversanne, I. Soerjomataram, A. Jemal, et al., Global cancer statistics 2020: GLOBOCAN estimates of incidence and mortality worldwide for 36 cancers in 185 countries, CA Cancer J. Clin. 71 (2021) 209–249, https://doi.org/10.3322/caac.21660.

[2] J.M. Llovet, R.K. Kelley, A. Villanueva, et al., Hepatocellular carcinoma, Nat. Rev. Dis. Primers 7 (1) (2021), 6, https://doi.org/10.1038/s41572-020-00240-3.
[3] W. Chen, R. Zheng, P.D. Baade, S. Zhang, H. Zeng, F. Bray, et al., Cancer statistics in China, 2015, CA Cancer J. Clin. 66 (2016) 115–132, https://doi.org/10.3322/caac.21338.
[4] A.S. Befeler, A.M. Di Bisceglie, Hepatocellular carcinoma: diagnosis and treatment, Gastroenterology 122 (2002) 1609–1619, https://doi.org/10.1053/gast.2002.33411.
[5] C. Allemani, T. Matsuda, V. Di Carlo, R. Harewood, M. Matz, M. Nikšić, et al., Global surveillance of trends in cancer survival 2000–14 (CONCORD-3): Analysis of individual records for 37 513 025 patients diagnosed with one of 18 cancers from 322 population-based registries in 71 countries, Lancet 391 (2018) 1023–1075, https://doi.org/10.1016/S0140-6736(17)33326-3.
[6] W. Sieghart, F. Hucke, M. Peck-Radosavljevic, Transarterial chemoembolization: modalities, indication, and patient selection, J. Hepatol. 62 (2015) 1187–1195, https://doi.org/10.1016/j.jhep.2015.02.010.
[7] Q.J. Li, M.K. He, H.W. Chen, W.Q. Fang, Y.M. Zhou, L. Xu, et al., Hepatic arterial infusion of oxaliplatin, fluorouracil, and leucovorin versus transarterial chemoembolization for large hepatocellular carcinoma: A randomized Phase III trial, J. Clin. Oncol. 40 (2022) 150–160, https://doi.org/10.1200/JCO.21.00608.
[8] L. Galluzzi, A. Buqué, O. Kepp, L. Zitvogel, G. Kroemer, Immunogenic cell death in cancer and infectious disease, Nat. Rev. Immunol. 17 (2017) 97–111, https://doi.org/10.1038/nri.2016.107.
[9] L. Galluzzi, I. Vitale, S. Warren, S. Adjemian, P. Agostinis, A.B. Martinez, et al., Consensus guidelines for the definition, detection and interpretation of immunogenic cell death, J. Immunother. Cancer 8 (2020), e000337, https://doi.org/10.1136/jitc-2019-000337.
[10] D.V. Krysko, A.D. Garg, A. Kaczmarek, O. Krysko, P. Agostinis, P. Vandenabeele, Immunogenic cell death and DAMPs in cancer therapy, Nat. Rev. Cancer 12 (2012) 860–875, https://doi.org/10.1038/nrc3380.
[11] J. Zhou, G. Wang, Y. Chen, H. Wang, Y. Hua, Z. Cai, Immunogenic cell death in cancer therapy: present and emerging inducers, J. Cell Mol. Med. 23 (2019) 4854–4865, https://doi.org/10.1111/jcmm.14356.
[12] J. Fucikova, O. Kepp, L. Kasikova, G. Petroni, T. Yamazaki, P. Liu, et al., Detection of immunogenic cell death and its relevance for cancer therapy, Cell Death Dis. 11 (2020), 1013, https://doi.org/10.1038/s41419-020-03221-2.
[13] M. Bian, R. Fan, Z. Yang, Y. Chen, Z. Xu, Y. Lu, W. Liu, Pt(II)-NHC complex induces ROS-ERS-related DAMP balance to harness immunogenic cell death in hepatocellular carcinoma, J. Med. Chem. 65 (3) (2022) 1848–1866, https://doi.org/10.1021/acs.jmedchem.1c01248.
[14] A. Tesniere, T. Panaretakis, O. Kepp, L. Apetoh, F. Ghiringhelli, L. Zitvogel, G. Kroemer, Molecular characteristics of immunogenic cancer cell death, Cell Death Differ. 15 (2008) 3–12, https://doi.org/10.1038/sj.cdd.4402269.
[15] J.J. Bednarski, B.P. Sleckman, At the intersection of DNA damage and immune responses, Nat. Rev. Immunol. 19 (2019) 231–242, https://doi.org/10.1038/s41577-019-0135-6.
[16] G. Sriram, L.E. Milling, J.K. Chen, Y.W. Kong, B.A. Joughin, W. Abraham, et al., The injury response to DNA damage in live tumor cells promotes antitumor immunity, Sci. Signal 14 (2021), eabc4764, https://doi.org/10.1126/scisignal.abc4764.
[17] Q. Storozynsky, M.M. Hitt, The impact of radiation-induced DNA damage on cGAS-STING-mediated immune responses to cancer, Int. J. Mol. Sci. 21 (2020), https://doi.org/10.3390/ijms21228877.
[18] P.H. Goff, R. Bhakuni, T. Pulliam, J.H. Lee, E.T. Hall, P. Nghiem, Intersection of two checkpoints: could inhibiting the DNA damage response checkpoint rescue immune checkpoint-refractory cancer? Cancers (Basel) 13 (2021), 3415 https://doi.org/10.3390/cancers13143415.
[19] B. Sangro, P. Sarobe, S. Hervás-Stubbs, I. Melero, Advances in immunotherapy for hepatocellular carcinoma, Nat. Rev. Gastroenterol. Hepatol. 18 (8) (2021) 525–543, https://doi.org/10.1038/s41575-021-00438-0.
[20] X. Huang, G. Zhang, T. Tang, T. Liang, Identification of tumor antigens and immune subtypes of pancreatic adenocarcinoma for mRNA vaccine development, Mol. Cancer 20 (2021), 44, https://doi.org/10.1186/s12943-021-01310-0.
[21] J. Lin, J. Shi, H. Guo, X. Yang, Y. Jiang, J. Long, et al., Alterations in DNA damage repair genes in primary liver cancer, Clin. Cancer Res. 25 (2019) 4701–4711, https://doi.org/10.1158/1078-0432.CCR-19-0127.
[22] Y. Chen, X. Wang, X. Deng, Y. Zhang, R. Liao, Y. Li, et al., DNA damage repair status predicts opposite clinical prognosis immunotherapy and non-immunotherapy in hepatocellular carcinoma, Front. Immunol. 12 (2021), 676922, https://doi.org/10.3389/fimmu.2021.676922.
[23] Y. Sun, E. Yin, Y. Tan, T. Yang, D. Song, S. Jin, et al., Immunogenicity and cytotoxicity of a platinum(IV) complex derived from capsaicin, Dalton Trans. 50 (2021) 3516–3522, https://doi.org/10.1039/d0dt03470c.
[24] A. Malik, U. Thanekar, S. Amarachintha, R. Mourya, S. Nalluri, A. Bondoc, P. Shivakumar, Complimenting the Complement": Mechanistic insights and opportunities for therapeutics in hepatocellular carcinoma, Front. Oncol. 10 (2020), 627701, https://doi.org/10.3389/fonc.2020.627701.
[25] A.K. Cotte, V. Aires, M. Fredon, E. Limagne, V. Derangère, M. Thibaudin, et al., Lysophosphatidylcholine acyltransferase 2-mediated lipid droplet production supports colorectal cancer chemoresistance, Nat. Commun. 9 (2018), 322, https://doi.org/10.1038/s41467-017-02732-5.
[26] A.M. Hammerquist, W. Escorcia, S.P. Curran, Maf1 regulates intracellular lipid homeostasis in response to DNA damage response activation, Mol. Biol. Cell 32 (2021) 1086–1093, https://doi.org/10.1091/mbc.E20-06-0378.
[27] H.G. Woo, X.W. Wang, A. Budhu, Y.H. Kim, S.M. Kwon, Z.Y. Tang, et al., Association of TP53 mutations with stem cell-like gene expression and survival of patients with hepatocellular carcinoma, Gastroenterology 140 (2011) 1063–1070, https://doi.org/10.1053/j.gastro.2010.11.034.
[28] Y. Zhao, C. Zhu, Q. Chang, J. Yang, Y. Liu, P. Peng, et al., TP53 rs28934571 polymorphism increases the prognostic risk in hepatocellular carcinoma, Biomark. Med. 15 (2021) 615–622, https://doi.org/10.2217/bmm-2020-0418.
[29] X. Xiao, H. Mo, K. Tu, CTNNB1 mutation suppresses infiltration of immune cells in hepatocellular carcinoma through miRNA-mediated regulation of chemokine expression, Int. Immunopharmacol. 89 (2020), 107043, https://doi.org/10.1016/j.intimp.2020.107043.
[30] L. Chen, Q. Zhou, J. Liu, W. Zhang, CTNNB1 alternation is a potential biomarker for immunotherapy prognosis in patients with hepatocellular carcinoma, Front. Immunol. 12 (2021), 759565, https://doi.org/10.3389/fimmu.2021.759565.
[31] M. Deldar Abad Paskeh, S. Mirzaei, M. Ashrafizadeh, A. Zarrabi, G. Sethi, Wnt/β-Catenin signaling as a driver of hepatocellular carcinoma progression: an emphasis on molecular pathways, J. Hepatocell. Carcinoma 8 (2021) 1415–1444, https://doi.org/10.2147/JHC.S336858.
[32] M. Felder, A. Kapur, J. Gonzalez-Bosquet, S. Horibata, J. Heintz, R. Albrecht, et al., MUC16 (CA125): Tumor biomarker to cancer therapy, a work in progress, Mol. Cancer 13 (2014), 129, https://doi.org/10.1186/1476-4598-13-129.
[33] C. Robert, A decade of immune-checkpoint inhibitors in cancer therapy, Nat. Commun. 11 (2020), 3801, https://doi.org/10.1038/s41467-020-17670-y.
[34] H. Sheng, Y. Huang, Y. Xiao, Z. Zhu, M. Shen, P. Zhou, et al., ATR inhibitor AZD6738 enhances the antitumor activity of radiotherapy and immune checkpoint inhibitors by potentiating the tumor immune microenvironment in hepatocellular carcinoma, J. Immunother. Cancer 8 (2020), https://doi.org/10.1136/jitc-2019-000340.
[35] E.B. Golden, L. Apetoh, Radiotherapy and immunogenic cell death, Semin. Radiat. Oncol. 25 (2015) 11–17, https://doi.org/10.1016/j.semradonc.2014.07.005.
[36] M.T. Dillon, K.F. Bergerhoff, M. Pedersen, H. Whittock, E. Crespo-Rodriguez, E. C. Patin, et al., ATR inhibition potentiates the radiation-induced inflammatory tumor microenvironment, Clin. Cancer Res. 25 (2019) 3392–3403, https://doi.org/10.1158/1078-0432.CCR-18-1821.
[37] L. D'Amico, U. Menzel, M. Prummer, P. Müller, M. Buchi, A. Kashyap, et al., A novel anti-HER2 anthracycline-based antibody-drug conjugate induces adaptive anti-tumor immunity and potentiates PD-1 blockade in breast cancer, J. Immunother. Cancer 7 (2019), 16, https://doi.org/10.1186/s40425-018-0464-1.
[38] T. Yamazaki, A. Buqué, T.D. Ames, L. Galluzzi, PT-112 induces immunogenic cell death and synergizes with immune checkpoint blockers in mouse tumor models, Oncoimmunology 9 (2020), 1721810, https://doi.org/10.1080/2162402X.2020.1721810.
[39] P. Schmid, S. Adams, H.S. Rugo, A. Schneeweiss, C.H. Barrios, H. Iwata, et al., Atezolizumab and nab-paclitaxel in advanced triple-negative breast cancer, N. Engl. J. Med. 379 (2018) 2108–2121, https://doi.org/10.1056/NEJMoa1809615.
[40] L. Horn, A.S. Mansfield, A. Szczęsna, L. Havel, M. Krzakowski, M.J. Hochmair, et al., First-line atezolizumab plus chemotherapy in extensive-stage small-cell lung cancer, N. Engl. J. Med. 379 (2018) 2220–2229, https://doi.org/10.1056/NEJMoa1809064.
[41] L. Gandhi, D. Rodríguez-Abreu, S. Gadgeel, E. Esteban, E. Felip, F. De Angelis, et al., Pembrolizumab plus chemotherapy in metastatic non-small-cell lung cancer, N. Engl. J. Med. 378 (2018) 2078–2092, https://doi.org/10.1056/NEJMoa1801005.
[42] W. Roh, P.L. Chen, A. Reuben, C.N. Spencer, P.A. Prieto, J.P. Miller, et al., Integrated molecular analysis of tumor biopsies on sequential CTLA-4 and PD-1 blockade reveals markers of response and resistance, Sci. Transl. Med. 9 (2017), https://doi.org/10.1126/scitranslmed.aah3560 eaah3560.
[43] A.B. Koenig, J.M. Barajas, M.J. Guerrero, K. Ghoshal, A comprehensive analysis of argonaute-CLIP data identifies novel, conserved and species-specific targets of miR-21 in human liver and hepatocellular Carcinoma, Int. J. Mol. Sci. 19 (3) (2018), 851, https://doi.org/10.3390/ijms19030851.
[44] X. Dai, W. Jiang, L. Ma, J. Sun, X. Yan, J. Qian, Y. Wang, Y. Shi, S. Ni, N. Yao, A metabolism-related gene signature for predicting the prognosis and therapeutic responses in patients with hepatocellular carcinoma, Ann. Transl. Med. 9 (6) (2021), 500, https://doi.org/10.21037/atm-21-927.
[45] N. Li, L. Zhao, C. Guo, C. Liu, Y. Liu, Identification of a novel DNA repair-related prognostic signature predicting survival of patients with hepatocellular carcinoma, Cancer Manag. Res. 11 (2019) 7473–7484, https://doi.org/10.2147/CMAR.S204864.
[46] Q. Li, B. Ren, Q. Gui, J. Zhao, M. Wu, M. Shen, D. Li, D. Li, K. Chen, M. Tao, R. Liang, Blocking MAPK/ERK pathway sensitizes hepatocellular carcinoma cells to temozolomide via downregulating MGMT expression, Ann. Transl. Med. 8 (20) (2020), 1305, https://doi.org/10.21037/atm-20-5478.
[47] Q. Meng, X. Duan, Q. Yang, D. Xue, Z. Liu, Y. Li, Q. Jin, F. Guo, S. Jia, Z. Wang, W. Yan, X. Chang, P. Sun, SLAMF6/Ly108 promotes the development of hepatocellular carcinoma via facilitating macrophage M2 polarization, Oncol. Lett. 23 (3) (2022), 83, https://doi.org/10.3892/ol.2022.13203.
[48] M. Wang, F. Jiang, K. Wei, J. Wang, G. Zhou, C. Wu, G. Yin, Development and validation of a RNA binding protein-associatedpPrognostic model for hepatocellular Carcinoma, Technol. Cancer Res. Treat. 20 (2021), 15330338211004936, https://doi.org/10.1177/15330338211004936.
[49] J. Zhang, X. Wang, C.J. Lin, F.J. Couch, P. Fei, Altered expression of FANCL confers Mitomycin C sensitivity in Calu-6 lung cancer cells, Cancer Biol. Ther. 5 (2006) 1632–1636, https://doi.org/10.4161/cbt.5.12.3351.
[50] Z.M. Zhao, S.E. Yost, K.E. Hutchinson, S.M. Li, Y.C. Yuan, J. Noorbakhsh, et al., CCNE1 amplification is associated with poor prognosis in patients with triple

negative breast cancer, BMC Cancer 19 (96) (2019), https://doi.org/10.1186/s12885-019-5290-4.